engineering proceedings

MDPI

Proceeding Paper

Catalytic Performance of Doped Ni_2P Surfaces for Ammonia Synthesis †

Abdulrahman Almithn

Department of Chemical Engineering, College of Engineering, King Faisal University, Al Ahsa 31982, Saudi Arabia; aalmithn@kfu.edu.sa

† Presented at the 4th International Electronic Conference on Applied Sciences, 27 October–10 November 2023; Available online: https://asec2023.sciforum.net/.

Abstract: Ammonia is a key ingredient in fertilizer production but its synthesis using the conventional Haber-Bosch process over metal-based catalysts is energy intensive. Prior investigations revealed that metal catalysts suffer from a trade-off between N_2 activation and N* binding strength, hindering their overall reactivity. Metal phosphide catalysts are promising alternatives to conventional metal catalysts due to their unique reactivity and stability. Here, we used DFT to study the catalytic performance of Ni_2P catalysts doped with Fe and Ru for ammonia synthesis. We show that H-assisted N–N activation may provide a new route to circumvent the N_2 dissociation scaling relationships.

Keywords: ammonia synthesis; nitrogen dissociation; nickel phosphide

1. Introduction

Ammonia (NH_3) holds a crucial position in various aspects of modern society. Its significance spans from agriculture to industry, making it an essential molecule for the global economy and sustainability efforts. It serves as a fundamental building block for the production of fertilizers, which are essential for enhancing crop yields and ensuring food security for a growing global population [1]. Additionally, ammonia finds applications in diverse sectors, including chemicals, pharmaceuticals, and even renewable energy storage. The Haber-Bosch process revolutionized agricultural productivity in the early 20th century by converting atmospheric nitrogen into ammonia over Fe-based catalysts and contributing to the large-scale production of synthetic fertilizers [2]. However, despite its immense importance, ammonia synthesis presents a range of formidable challenges.

The nitrogen (N_2) dissociation step is believed to be the rate limiting step in ammonia synthesis [3–6]. Cleaving the strong N≡N bond requires high temperatures and pressures over the conventional ammonia synthesis catalysts (Fe and Ru). The surface intermediates (NH_x; x = 0–3) formed during ammonia synthesis often bind too strongly to most transition metal catalysts under ambient conditions, thus elevated temperatures and pressures are necessary to maintain a favorable exergonic nature of the overall reaction [7]. The catalytic reduction of dinitrogen to ammonia under mild conditions is a long-standing challenge in catalysis. The goal is to find a catalyst that can bind NH_x species weakly while also maintaining a low energy barrier for N_2 dissociation. Computational assessments using density functional theory (DFT), however, have revealed a significant limitation: the N–N transition state energy cannot be adjusted without influencing the binding energy of NH_x to the surface, due to the presence of a Brønsted–Evans–Polanyi (BEP) scaling relationship for transition metal surfaces [8–11]. Decreasing the N_2 activation barrier also increases the binding strength of NH_x, thus hindering subsequent hydrogenation reactions and the production of NH_3. These studies have concluded that the turnover rate for ammonia synthesis as a function of N* binding energy for several transition metals

Citation: Almithn, A. Catalytic Performance of Doped Ni_2P Surfaces for Ammonia Synthesis. *Eng. Proc.* **2023**, *52*, x. https://doi.org/10.3390/xxxxx

Academic Editor(s): Name

Published: date

follows a volcano-shaped curve, with Fe and Ru being the only metals that are close to the optimum.

A logical approach to catalyst design was suggested, involving the combination of metals positioned on opposite sides of the volcano to achieve the desired interaction with nitrogen intermediates. For example, combining Co which binds N* too weakly with Mo which binds N* too strongly in the Co–Mo catalyst, leads to a material that has ammonia synthesis activity similar to that of Ru [12]. Many subsequent studies have focused on finding ways to circumvent the scaling relationship by using different catalytic materials, such as metal nitrides [13], hydrides [14], and oxides [15]. Electrochemical N_2 reduction has also emerged as an alternative approach for synthesizing NH_3 at ambient conditions, but the development of efficient electrochemical catalysts remains a key challenge [16–18]. Here, we explore the catalytic performance of Ni_2P catalyst doped with Fe and Ru for ammonia synthesis using DFT. We have previously shown that the incorporation of phosphorus atoms in nickel phosphide catalysts can alter the catalytic behavior of Ni atoms, leading to improved selectivity for various catalytic reactions [19–21]. The P atoms introduce weak binding surface sites that disrupt the metal ensembles. We also explore H-assisted N–N activation pathways involving diazene (N_2H_2) and hydrazine (N_2H_4) to weaken the N–N bond prior to activation.

2. Computational Methods

Periodic plane-wave DFT calculations were performed using the Vienna ab initio simulation package (VASP) [22–25], and the computational catalysis interface (CCI) [26]. The RPBE form of the generalized gradient approximation and PAW pseudopotentials were used [27–31]. The $Ni_2P(001)$ surface was constructed from bulk Ni_2P as described in more detail in our previous work [19]. Figure 1 shows the top and side views of the 2 × 2 $Ni_2P(001)$ surface used in this study. The bottom two atomic layers were constrained during geometric relaxation. Electronic energies were converged to within 10^{-6} eV, and forces were converged to less than 0.05 eVÅ^{-1} with a *k*-point mesh of 3 × 3 × 1 [32,33]. Transition state structures were identified using the nudged elastic band (NEB) method and the dimer method [34–36]. The $Ni_2P(001)$ surface was modified by substituting a surface Ni atom (highlighted in Figure 1a) with either Fe or Ru atom. This procedure mirrors the approach employed in a prior investigation using doped Ni_2P surfaces [37]. The formation energies of doped Ni_2P surfaces were calculated using the following formula:

$$E_f = E_{M/Ni2P} + E_{Ni} - E_{Ni2P} - E_M \quad (1)$$

where E_{Ni} and E_M are the energies of single Ni atom and single metal atom. The Ru–Ni_2P surface has a formation energy of −2.050 eV compared to −1.129 eV for Fe–Ni_2P, indicating that Ru–Ni_2P is more stable. Additional calculations were run using the pure 3 × 3 Fe(110) and Ru(001) surfaces for comparison. Spin-polarized calculations were exclusively applied to the Fe(110) and Fe–Ni_2P doped surfaces, as the energy discrepancy between spin-polarized and non-spin-polarized calculations exceeded 10^{-3} eV.

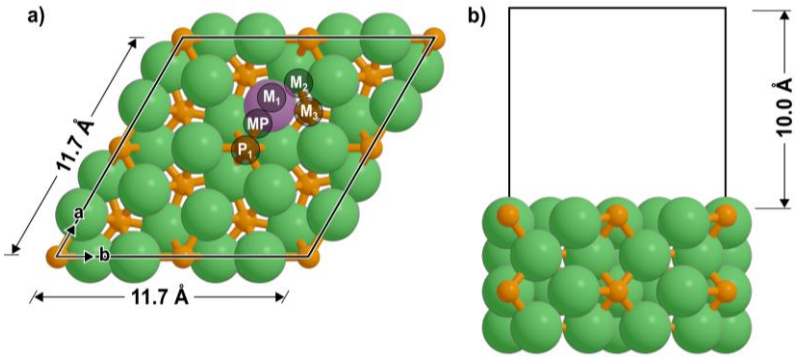

Figure 1. The top (**a**) and side (**b**) views of the doped $Ni_2P(001)$ surface model. Labels indicate different surface sites.

3. Results and Discussion

3.1. NH_x Species Binding Energies

In this section, we investigate the preferred adsorption configuration and binding energies of different NH_x species over Ni_2P, as well as doped Fe–Ni_2P and Ru–Ni_2P catalysts. For the sake of comparison, we also included the binding energies over pure Fe(110) and Ru(001) surfaces. Binding energies shown in Table 1 are calculated with respect to gas-phase species and bare surfaces (i.e., $\Delta E_{ads} = E_{species/surf} - E_{species(g)} - E_{surf}$). Diatomic nitrogen ($N_2$) vertically adsorbs on the metal atop site (M_1) over Ni_2P with a binding energy of −25 kJ mol^{-1}. This binding energy increases to −35 kJ mol^{-1} for Fe–Ni_2P and to −50 kJ mol^{-1} for Ru–Ni_2P. For NH_x* species, the binding strength increases as the number of hydrogen atoms bonded to the N atom decreases, i.e., NH_3* binds most weakly to the surface, whereas N* has the highest binding energy. This reflects the increasing stability of more saturated NH_x* species in the gas phase, and they coordinate with fewer metal atoms upon adsorption. For example, N* and NH* bind to the metal 3-fold (M_3) site whereas NH_2 and NH_3 bind to the bridging (M_2) and atop (M_1) sites, respectively (Figure 2).

Table 1. The binding energies (ΔE_{ads} in kJ mol^{-1}) of N_2*, H*, and NH_x (x = 0–3) over the catalytic surfaces examined in this study.

	$Ni_2P(001)$		Fe–$Ni_2P(001)$		Ru–$Ni_2P(001)$		Fe(110)		Ru(001)	
Species	**Mode**	**ΔE_{ads}**	**Mode**	**ΔE_{ads}**	**Mode**	**ΔE_{ads}**	**Mode**	**ΔE_{ads}**	**Mode**	**ΔE_{ads}**
N_2*	M_1	−25	M_1	−35	M_1	−50	M_1	−95	M_1	−34
H*	M_3	−222	M_3	−240	M_3	−246	M_3	−288	M_3	−262
N*	M_3	−375	M_3	−435	M_3	−445	M_4	−601	M_3	−551
NH*	M_3	−325	M_3	−353	M_3	−365	M_3	−528	M_3	−437
NH_2*	M_2	−224	M_2	−235	M_2	−256	M_2	−326	M_3	−213
NH_3*	M_1	−60	M_1	−50	M_1	−74	M_1	−109	M_1	−63

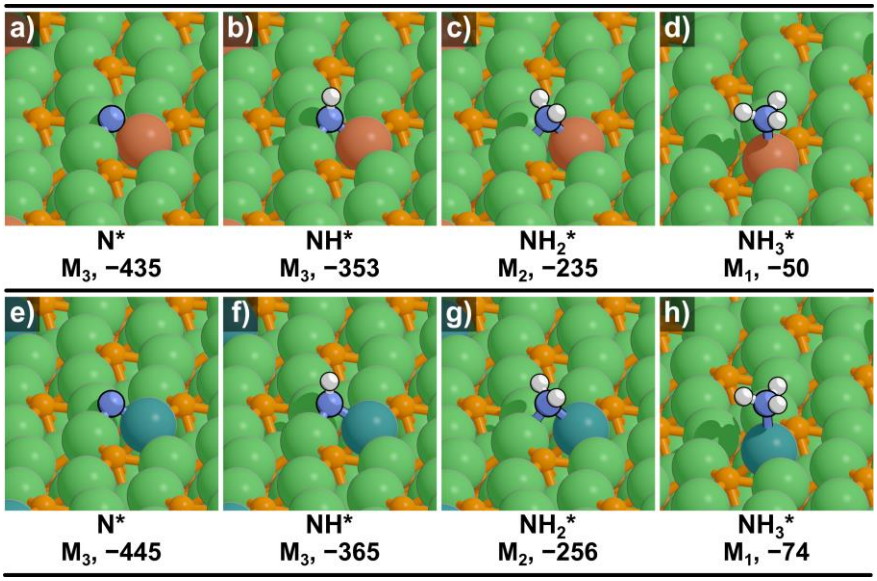

Figure 2. Adsorbed NH_x (x = 0–3) species over Fe–Ni_2P (**a**–**d**) and Ru–Ni_2P (**e**–**h**) catalysts. The adsorption configuration and binding energies (ΔE_{ads} in kJ mol^{-1}) are shown beneath each image.

We also observe a general trend in binding energies across examined surfaces where the binding strength for each species generally increases as Ni_2P → Fe–Ni_2P → Ru–Ni_2P → Ru → Fe with few exceptions. If we consider the N* binding energy as a proxy for the

catalytic activity towards N–N bond activation within N_2, following the principles of Brønsted–Evans–Polanyi (BEP) scaling relations [8–11], it can be inferred that Ni_2P is likely to exhibit weak activity. Conversely, Fe and Ru doped Ni_2P catalysts are expected to demonstrate higher activity compared to pure Ni_2P, although falling short of the reactivity of Fe- and Ru-based catalysts. However, this also means that Fe- and Ru-based catalysts are more prone to deactivation due to the strongly bound N* or NH* than phosphide-based catalysts.

3.2. N–N Activation Reactions

Here, we examine the N–N bond cleavage reactions in N_2*, N_2H_2*, and N_2H_4* as shown in Figure 3. Over the Ru(001) surface, adsorbed N_2* undergoes N–N bond activation with a forward activation barrier (ΔE_a) of 168 kJ mol^{-1} to form two nitrogen atoms (2N*) both adsorbed on separate 3-fold sites. This reaction is slightly endothermic with a reaction energy (ΔE_{rxn}) of 13 kJ mol^{-1}. These results are consistent with previous studies on Ru(001) flat surfaces [38]. On both Fe-Ni_2P and Ru-Ni_2P surfaces, N_2* dissociates to 2N* with a much larger activation barrier of 350 kJ mol^{-1} and a highly endothermic reaction energy. This reaction starts with N_2* vertically adsorbed on the doped metal atom. After the N–N bond cleavage, the N* atoms bind to nearby 3-fold sites. We have attempted this reaction and even the other H-assisted N–N bond activation reactions in N_2H_2 and N_2H_4 over the undoped Ni_2P surface, but we were not able to identify stable transition states. The trends in N* binding energy discussed in Section 3.1 indeed correlate with the calculated N–N bond activation barriers over these materials.

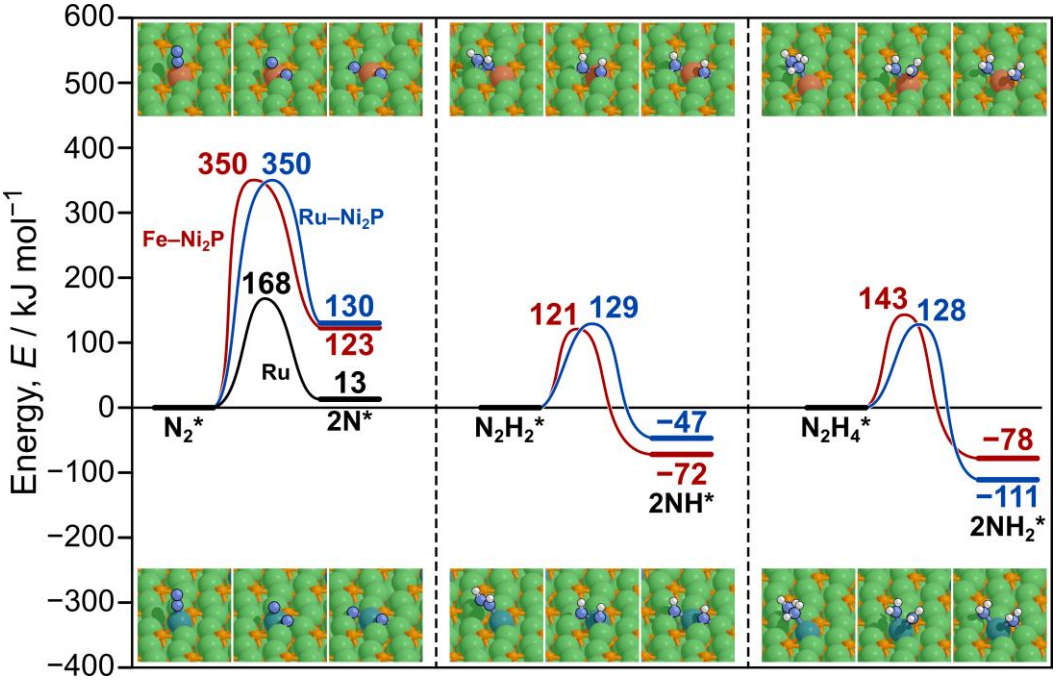

Figure 3. Reaction coordinate diagram for N–N bond activation in N_2*, N_2H_2*, and N_2H_4* over Fe–Ni_2P (red), Ru–Ni_2P (blue), and Ru (black). Images display the reactants, transition state, and products structures over Fe–Ni_2P (top) and Ru–Ni_2P (bottom).

We next examine the N–N bond activation reactions in diazine (N_2H_2) and hydrazine (N_2H_4) to investigate whether hydrogenating N_2 can weaken the N–N bond prior to its activation. Figure 3 shows that the activation barrier of the N–N bond in adsorbed N_2H_2* dramatically decreased by more than 220 kJ mol^{-1} over both Fe–Ni_2P and Ru–Ni_2P surfaces (121 and 129 kJ mol^{-1}, respectively) compared to direct N_2* dissociation (350 kJ mol^{-1}). Breaking the N–N bond in N_2H_4 also exhibits a similar barrier of 128 kJ mol^{-1} over Ru-Ni_2P, but the barrier for this reaction over Fe-Ni_2P increases to 143 kJ mol^{-1}. We expect a

similar decrease in the activation barrier of H-assisted N–N activation over pure Ru(001) surface, however, the resulting NH* also strongly binds to the surface (Table 1) which may render the active sites inert. The more facile activation of N–N bond in N_2H_2* over both Fe-Ni_2P and Ru-Ni_2P doped surfaces, coupled with the weaker binding of the product NH*, may open the door for a promising pathway which avoids the current paradigm of direct N_2 dissociation. However, it is important to note that further analysis of the hydrogenation reactions to produce N_2H_2 and eventually NH_3 over these materials is necessary to fully ascertain the viability of this pathway.

4. Conclusions

In this work, we investigated the binding energies of various NH_x species and the N–N bond activation energy over Ni_2P catalysts doped with Fe and Ru using DFT. Our results indicate that NH_x species with fewer hydrogen atoms bind more strongly to the catalytic surfaces, and the binding strength generally increases as Ni_2P → Fe–Ni_2P → Ru–Ni_2P → Ru → Fe. This trend is reflected in the relative activity of these catalytic surfaces towards direct N_2* dissociation with Ru being the most active and Ni_2P the least active surface. However, we show that hydrogenating the N_2* prior to N–N bond cleavage can dramatically decrease the activation barrier over doped Ni_2P surfaces. These findings suggest that the H-assisted N–N bond activation may play a crucial role in reducing the activation energy required for ammonia synthesis over these surfaces without concomitant increase in binding strength of NH_x species. Further investigation into the underlying mechanisms of this catalytic process could potentially lead to enhanced strategies for nitrogen activation and ammonia synthesis.

Funding: This research received no external funding.

Institutional Review Board Statement:

Informed Consent Statement:

Data Availability Statement:

Conflicts of Interest: The author declares no conflict of interest.

References

1. Erisman, J.W.; Sutton, M.A.; Galloway, J.; Klimont, Z.; Winiwarter, W. How a Century of Ammonia Synthesis Changed the World. *Nat. Geosci.* **2008**, *1*, 636–639. https://doi.org/10.1038/ngeo325.
2. Smil, V. *Enriching the Earth: Fritz Haber, Carl Bosch, and the Transformation of World Food Production*; MIT Press: Cambridge, MA, USA, 2004; ISBN 0262693135.
3. Boudart, M. Kinetics and Mechanism of Ammonia Synthesis. *Catal. Rev.* **1981**, *23*, 1–15. https://doi.org/10.1080/03602458108068066.
4. Honkala, K.; Hellman, A.; Remediakis, I.N.; Logadottir, A.; Carlsson, A.; Dahl, S.; Christensen, C.H.; Nørskov, J.K. Ammonia Synthesis from First-Principles Calculations. *Science* **2005**, *307*, 555–558. https://doi.org/10.1126/science.1106435.
5. Schlögl, R. Catalytic Synthesis of Ammonia—A "Never-Ending Story"? *Angew. Chem. Int. Ed.* **2003**, *42*, 2004–2008. https://doi.org/10.1002/anie.200301553.
6. Ertl, G. Surface Science and Catalysis—Studies on the Mechanism of Ammonia Synthesis: The P. H. Emmett Award Address. *Catal. Rev.* **1980**, *21*, 201–223. https://doi.org/10.1080/03602458008067533.
7. Vojvodic, A.; Medford, A.J.; Studt, F.; Abild-Pedersen, F.; Khan, T.S.; Bligaard, T.; Nørskov, J.K. Exploring the Limits: A Low-Pressure, Low-Temperature Haber-Bosch Process. *Chem. Phys. Lett.* **2014**, *598*, 108–112. https://doi.org/10.1016/j.cplett.2014.03.003.
8. Logadottir, A.; Rod, T.H.; Nørskov, J.K.; Hammer, B.; Dahl, S.; Jacobsen, C.J.H. The Brønsted-Evans-Polanyi Relation and the Volcano Plot for Ammonia Synthesis over Transition Metal Catalysts. *J. Catal.* **2001**, *197*, 229–231. https://doi.org/10.1006/jcat.2000.3087.
9. Munter, T.R.; Bligaard, T.; Christensen, C.H.; Nørskov, J.K. BEP Relations for N2 Dissociation over Stepped Transition Metal and Alloy Surfaces. *Phys. Chem. Chem. Phys.* **2008**, *10*, 5202. https://doi.org/10.1039/b720021h.
10. Nørskov, J.K.; Bligaard, T.; Hvolbæk, B.; Abild-Pedersen, F.; Chorkendorff, I.; Christensen, C.H. The Nature of the Active Site in Heterogeneous Metal Catalysis. *Chem. Soc. Rev.* **2008**, *37*, 2163. https://doi.org/10.1039/b800260f.

11. Medford, A.J.; Vojvodic, A.; Hummelshøj, J.S.; Voss, J.; Abild-Pedersen, F.; Studt, F.; Bligaard, T.; Nilsson, A.; Nørskov, J.K. From the Sabatier Principle to a Predictive Theory of Transition-Metal Heterogeneous Catalysis. *J. Catal.* **2015**, *328*, 36–42. https://doi.org/10.1016/j.jcat.2014.12.033.
12. Jacobsen, C.J.H.; Dahl, S.; Clausen, B.G.S.; Bahn, S.; Logadottir, A.; Nørskov, J.K. Catalyst Design by Interpolation in the Periodic Table: Bimetallic Ammonia Synthesis Catalysts. *J. Am. Chem. Soc.* **2001**, *123*, 8404–8405.
13. Zeinalipour-Yazdi, C.D.; Hargreaves, J.S.J.; Catlow, C.R.A. Nitrogen Activation in a Mars–van Krevelen Mechanism for Ammonia Synthesis on Co_3Mo_3N. *J. Phys. Chem. C* **2015**, *119*, 28368–28376. https://doi.org/10.1021/acs.jpcc.5b06811.
14. Wang, P.; Chang, F.; Gao, W.; Guo, J.; Wu, G.; He, T.; Chen, P. Breaking Scaling Relations to Achieve Low-Temperature Ammonia Synthesis through LiH-Mediated Nitrogen Transfer and Hydrogenation. *Nat. Chem.* **2017**, *9*, 64–70. https://doi.org/10.1038/nchem.2595.
15. Vojvodic, A.; Calle-Vallejo, F.; Guo, W.; Wang, S.; Toftelund, A.; Studt, F.; Martínez, J.I.; Shen, J.; Man, I.C.; Rossmeisl, J.; et al. On the Behavior of Brønsted-Evans-Polanyi Relations for Transition Metal Oxides. *J. Chem. Phys.* **2011**, *134*, 244509. https://doi.org/10.1063/1.3602323.
16. Choi, C.; Back, S.; Kim, N.-Y.; Lim, J.; Kim, Y.-H.; Jung, Y. Suppression of Hydrogen Evolution Reaction in Electrochemical N_2 Reduction Using Single-Atom Catalysts: A Computational Guideline. *ACS Catal.* **2018**, *8*, 7517–7525. https://doi.org/10.1021/acscatal.8b00905.
17. Liu, C.; Li, S.; Li, Z.; Zhang, L.; Chen, H.; Zhao, D.; Sun, S.; Luo, Y.; Alshehri, A.A.; Hamdy, M.S.; et al. Ambient N_2-to-NH_3 Fixation over a CeO_2 Nanoparticle Decorated Three-Dimensional Carbon Skeleton. *Sustain. Energy Fuels* **2022**, *6*, 3344–3348. https://doi.org/10.1039/D2SE00557C.
18. Wang, F.; Zhang, L.; Wang, T.; Zhang, F.; Liu, Q.; Zhao, H.; Zheng, B.; Du, J.; Sun, X. In Situ Derived Bi Nanoparticles Confined in Carbon Rods as an Efficient Electrocatalyst for Ambient N_2 Reduction to NH_3. *Inorg. Chem.* **2021**, *60*, 7584–7589. https://doi.org/10.1021/acs.inorgchem.1c01130.
19. Witzke, M.E.; Almithn, A.; Conrad, C.L.; Hibbitts, D.D.; Flaherty, D.W. Mechanisms and Active Sites for C–O Bond Rupture within 2-Methyltetrahydrofuran over Ni, $Ni_{12}P_5$, and Ni_2P Catalysts. *ACS Catal.* **2018**, *8*, 7141–7157. https://doi.org/10.1021/acscatal.7b04403.
20. Almithn, A.; Alhulaybi, Z. A Mechanistic Study of Methanol Steam Reforming on Ni2P Catalyst. *Catalysts* **2022**, *12*, 1174. https://doi.org/10.3390/catal12101174.
21. Almithn, A.; Alghanim, S.N.; Mohammed, A.A.; Alghawinim, A.K.; Alomaireen, M.A.; Alhulaybi, Z.; Hossain, S.S. Methane Activation and Coupling Pathways on Ni2P Catalyst. *Catalysts* **2023**, *13*, 531. https://doi.org/10.3390/catal13030531.
22. Kresse, G.; Hafner, J. Ab Initio Molecular Dynamics for Liquid Metals. *Phys. Rev. B* **1993**, *47*, 558–561. https://doi.org/10.1103/PhysRevB.47.558.
23. Kresse, G.; Hafner, J. Ab Initio Molecular-Dynamics Simulation of the Liquid-Metal–Amorphous-Semiconductor Transition in Germanium. *Phys. Rev. B* **1994**, *49*, 14251–14269. https://doi.org/10.1103/PhysRevB.49.14251.
24. Kresse, G.; Furthmüller, J. Efficient Iterative Schemes for Ab Initio Total-Energy Calculations Using a Plane-Wave Basis Set. *Phys. Rev. B* **1996**, *54*, 11169–11186. https://doi.org/10.1103/PhysRevB.54.11169.
25. Kresse, G.; Furthmüller, J. Efficiency of Ab-Initio Total Energy Calculations for Metals and Semiconductors Using a Plane-Wave Basis Set. *Comput. Mater. Sci.* **1996**, *6*, 15–50. https://doi.org/10.1016/0927-0256(96)00008-0.
26. Kravchenko, P.; Plaisance, C.; Hibbitts, D. A New Computational Interface for Catalysis. *ChemRxiv* 2019, *preprint*.
27. Hammer, B.; Hansen, L.B.; Nørskov, J.K. Improved Adsorption Energetics within Density-Functional Theory Using Revised Perdew-Burke-Ernzerhof Functionals. *Phys. Rev. B* **1999**, *59*, 7413–7421. https://doi.org/10.1103/PhysRevB.59.7413.
28. Perdew, J.P.; Burke, K.; Ernzerhof, M. Generalized Gradient Approximation Made Simple. *Phys. Rev. Lett.* **1996**, *77*, 3865–3868. https://doi.org/10.1103/PhysRevLett.77.3865.
29. Zhang, Y.; Yang, W. Comment on "Generalized Gradient Approximation Made Simple." *Phys. Rev. Lett.* **1998**, *80*, 890–890. https://doi.org/10.1103/PhysRevLett.80.890.
30. Blöchl, P.E. Projector Augmented-Wave Method. *Phys. Rev. B* **1994**, *50*, 17953–17979. https://doi.org/10.1103/PhysRevB.50.17953.
31. Kresse, G.; Joubert, D. From Ultrasoft Pseudopotentials to the Projector Augmented-Wave Method. *Phys. Rev. B* **1999**, *59*, 1758–1775. https://doi.org/10.1103/PhysRevB.59.1758.
32. Monkhorst, H.J.; Pack, J.D. Special Points for Brillouin-Zone Integrations. *Phys. Rev. B* **1976**, *13*, 5188–5192. https://doi.org/10.1103/PhysRevB.13.5188.
33. Pack, J.D.; Monkhorst, H.J. "Special Points for Brillouin-Zone Integrations"—A Reply. *Phys. Rev. B* **1977**, *16*, 1748–1749. https://doi.org/10.1103/PhysRevB.16.1748.
34. Henkelman, G.; Jónsson, H. Improved Tangent Estimate in the Nudged Elastic Band Method for Finding Minimum Energy Paths and Saddle Points. *J. Chem. Phys.* **2000**, *113*, 9978–9985. https://doi.org/10.1063/1.1323224.
35. Henkelman, G.; Jónsson, H. A Dimer Method for Finding Saddle Points on High Dimensional Potential Surfaces Using Only First Derivatives. *J. Chem. Phys.* **1999**, *111*, 7010–7022. https://doi.org/10.1063/1.480097.
36. Jónsson, H.; Mills, G.; Jacobsen, K.W. Nudged Elastic Band Method for Finding Minimum Energy Paths of Transitions. *In Classical and Quantum Dynamics in Condensed Phase Simulations*; World Scientific: Singapore, 1998; pp. 385–404.
37. Wang, G.; Shi, Y.; Mei, J.; Xiao, C.; Hu, D.; Chi, K.; Gao, S.; Duan, A.; Zheng, P. DFT Insights into Hydrogen Activation on the Doping Ni2P Surfaces under the Hydrodesulfurization Condition. *Appl. Surf. Sci.* **2021**, *538*, 148160. https://doi.org/10.1016/j.apsusc.2020.148160.

38. Dahl, S.; Logadottir, A.; Egeberg, R.C.; Larsen, J.H.; Chorkendorff, I.; Törnqvist, E.; Nørskov, J.K. Role of Steps in N2 Activation on Ru(0001). *Phys. Rev. Lett.* **1999**, *83*, 1814–1817. https://doi.org/10.1103/PhysRevLett.83.1814.